

Dimensionality Dependence of the Band-Gap Renormalization in Two- and Three-Dimensional Electron-Hole Plasmas in GaAs

G. Tränkle, H. Leier, and A. Forchel

4. Physikalisches Institut, Universität Stuttgart, D-7000 Stuttgart 80, Federal Republic of Germany

H. Haug and C. Ell

Institut für Theoretische Physik, Universität Frankfurt, D-6000 Frankfurt, Federal Republic of Germany

and

G. Weimann

Forschungsinstitut der Bundespost, D-6100 Darmstadt, Federal Republic of Germany

(Received 27 May 1986)

We have investigated the band-gap renormalization due to many-body effects in electron-hole plasmas in 2D GaAs-GaAlAs multiple quantum-well structures. A comparison of these data with corresponding 3D data and calculations for both dimensionalities shows that the band-gap shift increases absolutely but decreases in effective Rydberg units with decreasing dimensionality. The dimensionality dependence of the band-gap shift is traced to different screening efficiencies in 3D and 2D systems.

PACS numbers: 71.35.+z, 73.40.Lq

Many-body effects in dense electron-hole plasmas (EHP) in intrinsic semiconductors lead to a renormalization of the fundamental band gap. In three-dimensional (3D) semiconductor structures this effect is quantitatively understood. A key result is the universal law of the plasma-density dependence on the band-gap renormalization. Scaled in the appropriate units of the materials (effective Rydberg energy and Bohr radius) this relation is independent of the band structure or other material properties.^{1,2}

Up to now there have been no systematic experimental investigations on the relation between the carrier density and the band-gap renormalization in quasi two-dimensional (2D) structures. Transmission³ and photoluminescence^{4,5} measurements yielded only qualitative results. In this paper we report high-excitation photoluminescence measurements in GaAs-GaAlAs multiple-quantum-well (MQW) structures at low temperatures ($T_{\text{lattice}} \approx 2$ K) and determine for the first time the quantitative relationship between the band-gap shift and the carrier density in the 2D EHP. The experimental results are compared with numerical and analytical^{6,7} calculations of the band-gap renormalization. We observe in 2D EHP much larger absolute band-gap shifts than those which have been observed in 3D EHP.⁸ However, if the band-gap shifts are scaled in the natural energy units, namely the appropriate 2D and 3D Rydberg energies, our results show that the 2D band-gap shift is effectively smaller because of the reduced efficiency of screening in 2D EHP.

In our experiment we used high-quality GaAs-Ga_{0.57}Al_{0.43}As MQW structures grown by molecular-beam epitaxy. They consisted of about 25 GaAs layers with well widths L_z between 21 and 83 Å. The thickness

of the barriers L_B was about 180 Å to avoid coupling between adjacent wells. We characterized the quasi-2D systems by excitation spectroscopy and obtained transition energies of the free excitons at the subband edges. From the lowest excitonic transition between the first electron subband and the first heavy-hole subband we have determined the fundamental band edge in the quantum wells at zero density by use of experimental values for the excitonic binding energy determined by Maan *et al.*⁹

In the high-excitation measurements the plasma was generated with a pulsed dye laser. The pulse duration was $\tau_{\text{laser}} \approx 10$ ns, much larger than typical relaxation times in GaAs-GaAlAs QW structures. Therefore we assume a quasistationary excitation of our samples permitting a quasiequilibrium description of the EHP. In Fig. 1 we depict photoluminescence spectra for a sample with a well width of 21 Å. With increasing excitation power we observe a strong shift of the low-energy edge of the spontaneous QW luminescence to lower energies (up to 35 meV) and the spectra broaden drastically, clearly indicating the formation of a high-density EHP. At the highest excitation intensities even the center of the luminescence band shifts to lower energies.

In order to obtain the plasma density, temperature, and renormalized band gap we performed a line-shape analysis in a simple 2D model⁵: Electrons and holes are distributed in parabolic subbands with a steplike 2D density of states. The subband energies are calculated for a rectangular potential well with finite barriers on the basis of the results of the excitation spectroscopy.

We approximated the realistic nonparabolic valence-band dispersion¹⁰ by using the bulk effective masses of heavy and light holes. By comparison with calculated

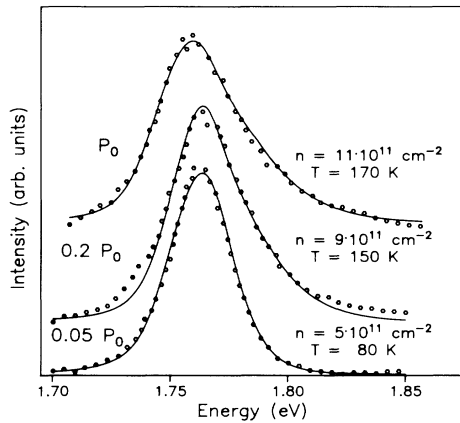


FIG. 1. Luminescence spectra and line-shape fits (solid lines) for a sample of $L_z = 21 \text{ \AA}$ as functions of the excitation intensity. ($P_0 \approx 500 \text{ kW/cm}^2$.)

dispersion relations it can be shown that these bulk values give a good approximation of the exact values. This is a consequence of the large band filling in the present investigations.¹¹ Furthermore, we assumed common quasichemical potentials for the subbands of the electrons and of the holes, respectively, and a common temperature for all carriers.

With the assumption of momentum conservation for the optical transition and a constant matrix element, the luminescence spectrum is then given by

$$I(\hbar\omega) \propto \sum_{ij} \int_{E_i^0}^{\infty} \int_{E_j^0}^{\infty} m_i m_j f_e(E_i) f_h(E_j) \times \delta_{\gamma}(E_i + E_j - \hbar\omega) dE_i dE_j. \quad (1)$$

The indices i, j denote the electron and hole subbands, respectively. $E_{i,j}$ are the subband energies, $m_{i,j}$ are the masses, and $f_{e,h}$ are the Fermi distributions of the electrons and holes. For allowed transitions Eq. (1) is limited by the usual selection rule ($i = j$). The common quasichemical potentials μ , e.g., for the electrons, are given by the relation

$$n = \frac{kT}{\pi \hbar^2} \sum m_i \ln \left[1 + \exp \left(\frac{\mu_e - E_i}{kT} \right) \right]. \quad (2)$$

δ_{γ} is a broadened delta function. If the spectra are calculated from (1) and (2) without any broadening they deviate from the experimental data at the low-energy edge. Therefore we took a collision broadening γ into account phenomenologically in the form suggested by Landsberg.¹² This energy broadening γ has a maximum at the band edge and vanishes at the chemical potential. It does not affect the linewidth of the spectra, which is a measure of the EHP density.

The solid lines of Fig. 1 are typical results of our line-shape analysis with use of 3D masses ($m_{hh} = 0.45m_e$, $m_{lh} = 0.08m_e$) in the calculations. The agreement be-

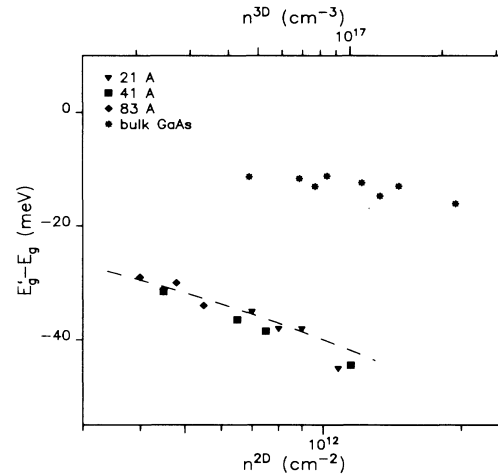


FIG. 2. Measured density dependence of the band-gap renormalization for various GaAs-GaAlAs MQW structures and for bulk GaAs (Ref. 8). The density axes are comparable because they are based on the dimensionless interparticle distance r_s . The 2D band-gap renormalization depends on the density proportional to $n_{2D}^{1/3}$ as expected theoretically (Ref. 6) (dashed line).

tween the experimental data and the fitted curves is very reasonable. Plasma temperatures between 60 and 170 K are observed under high excitation conditions. The excess energy of the carriers resulting from the non-resonant excitation ($\hbar\omega_{\text{laser}} \approx 2 \text{ eV}$) is not transferred completely to the lattice under the experimental conditions, especially in 2D structures where reduced carrier cooling rates are observed.¹³

From the line-shape fits we obtained the plasma densities and the renormalized band edges in the high-density plasma. Since we have determined the zero-density band edge from the excitation spectra by correcting for the exciton binding energy using recent experimental results⁷ we were now able to determine the density dependence of the band-gap renormalization.

In Fig. 2 we depict the band-gap shift as a function of the 2D plasma density for the well widths of $L_z = 21, 41,$ and 83 \AA . For comparison we include data measured previously in 3D GaAs structures under comparable experimental conditions.⁶ The relation of the density axes of the 2D and 3D plasmas is based on equivalent interparticle distances r_s , obtained from $\pi r_s^2 = (n a_{02D}^2)^{-1}$ and $4\pi r_s^3/3 = (n a_{03D}^3)^{-1}$, respectively. For the Bohr radii we obtained in 2D a value of $a_{02D} = 57 \text{ \AA}$ (corresponding to a mass of $0.45m_0$; see Ref. 14) and in 3D⁸ a value of $a_{03D} = 146 \text{ \AA}$. Figure 2 displays two important results:

(i) For the same interparticle distance the band-gap renormalization in the 2D plasma is significantly larger than in the 3D plasma. We measure shifts of the band edge between 25 and 45 meV for the 2D plasma, whereas in the 3D case the shifts are below 20 meV for

all densities. The large absolute values of the band-gap shift in 2D systems can be understood qualitatively by the increase of the Rydberg energy by a factor of about 4 compared to the 3D case. As has been shown previously^{1,8} for 3D systems the band-gap renormalization is approximately proportional to the Rydberg energy.

(ii) Within the experimental accuracy we observe no well-width dependence of the band-gap renormalization in the MQW structures. This is a strong indication that the 2D limit is reached in all our samples.

The appropriately scaled experimental results for 2D and 3D⁸ GaAs are compared with numerical calculations of the band-gap shrinkage ΔE_g in Fig. 3. The energies in both cases are scaled with the corresponding Rydberg energies, E_{02D} (Ref. 14) and E_{03D} , respectively. For the experimental and theoretical GaAs-GaAlAs MQW results we used a value of $E_{02D} = 19.9$ meV. The experimental bulk GaAs values are scaled by⁸ $E_{03D} = 3.9$ meV.

The 2D self-energies have been calculated in the dynamical random-phase approximation (RPA) with a single-plasmon pole approximation⁶ (SPP). The results have been the same as those obtained from the dynamical RPA. It is known that in 2D short-range correlations are more important and the RPA is less satisfying than in 3D.¹⁵ In order to investigate the influence of short-range correlations we also calculated the 2D self-energies in a Hubbard modified RPA in which the intra-band dielectric function^{16,17} is given by

$$\epsilon(q, \omega) = \epsilon_0 \left[1 - \sum_{i=e,h} \frac{P_i(q, \omega)}{1 + \frac{1}{2} [q/(q+k_F)] P_i(q, \omega)} \right], \quad (3)$$

where

$$P_i(q, \omega) = 2V_q \sum_{\mathbf{k}} \frac{f_i(\mathbf{k}) - f_i(\mathbf{k}+\mathbf{q})}{\omega - \epsilon_{i\mathbf{k}+\mathbf{q}} + \epsilon_{i\mathbf{k}} + i\delta}, \quad (4)$$

with

$$V_q = \frac{2\pi e^2}{\epsilon_0 q}, \quad f_i(k) = \frac{1}{\exp[\beta(\epsilon_{ik} - \mu_i)] + 1},$$

and

$$\epsilon_{ik} = k^2/2m_i \quad (i=e,h). \quad (5)$$

In Fig. 3 we compare the results of the SPP with the Hubbard modified RPA for $T=0$ K and equal electron and hole masses. The deviation between the calculations is small indicating that the influence of the short-range correlations is small in the investigated density range. In addition, we calculated the 2D self-energies within the dynamical SPP for the electron and hole masses of bulk GaAs and a temperature of 150 K. In 3D the SPP is known to yield⁷ results which are close to the universal law of Vashishta and Kalia,¹ which is also shown in Fig. 3 as a dashed line.

Figure 3 clearly shows that in the universal units Ryd-

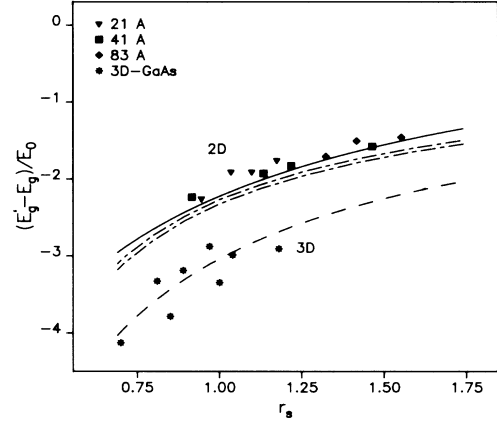


FIG. 3. Band-gap shift ΔE_g scaled by the 2D and 3D Rydberg energies vs the dimensionless interparticle distance r_s for 2D and 3D (Ref. 8) GaAs structures. The numerical results for a 2D plasma are calculated in a dynamical RPA with a single-plasmon pole approximation (upper dot-dashed line: $m_e = m_h$, $T=0$ K; full line: m_e, m_h bulk values, $T=150$ K) and in a Hubbard-modified RPA (lower dot-dashed line: $m_e = m_h$, $T=0$ K). The universal 3D law (Ref. 1) is given by the dashed line.

berg energy and Bohr radius both experiment and theory yield a band-gap shrinkage in 2D systems which is considerably smaller than in the bulk material for the same interparticle distance. The absolute values for the scaled theoretical and experimental band-gap shifts agree quantitatively for both dimensions.

In order to get a better understanding of the results of Fig. 3 we discuss the asymptotic behavior of the band-gap renormalization by calculating the self-energies in the Debye limit analytically. In this classical low-density limit band-filling effects are neglected, so that ΔE_g is simply the self-energy of a point charge in the plasma: $\Delta E_g = \sum_{\mathbf{k}} (V_{s\mathbf{k}} - V_{\mathbf{k}}) = V_s(r) - V(r)$ for $r \rightarrow 0$, where V_s is the statically screened Coulomb potential. The band gap shrinks because the Coulomb potential is weakened by the screening in the plasma. In 2D where $V_k = 2\pi e^2/\epsilon_0 k$ and $V_{sk} = V_k [k/(k+k_{s2D})]$, one has to introduce a cutoff $k_c = kT\epsilon_0/e^2$ for the closest approach of the two thermal electrons or holes, which takes into account the short-range correlations. In the Debye limit the 2D band-gap shift is thus given by

$$\Delta E_{g2D} = -\frac{e^2 k_{s2D}}{\epsilon_0} \ln \left[1 + \frac{k_c}{k_{s2D}} \right]. \quad (6)$$

In 3D, where $V_s(r) = (e^2/\epsilon_0 r) \exp(-rk_{s3D})$, the band-gap shift is thus

$$\Delta E_{g3D} = -e^2 k_{s3D}/\epsilon_0. \quad (7)$$

The Debye screening wave numbers are given by $k_{s2D} = 4\pi n e^2/\epsilon_0 kT$ and $k_{s3D} = (8\pi n e^2/\epsilon_0 kT)^{1/2}$. The re-

sulting scaled 3D and 2D gap shifts are

$$\frac{\Delta E_{g2D}}{E_{02D}} = -4 \left(\frac{E_{02D}}{kT} \right) r_s^{-2} \ln \left[1 + \frac{r_s^2 (kT)^2}{4E_{02D}^2} \right], \quad (8)$$

$$\frac{\Delta E_{g3D}}{E_{03D}} = -4 \left(\frac{3E_{03D}}{kT} \right)^{1/2} r_s^{-3/2}. \quad (9)$$

In the Debye limit $r_s \gg 1$ the scaled 2D band-gap shift is dominated by the factor r_s^{-2} . Therefore it is smaller than the corresponding 3D result which indicates the reduced efficiency of screening. At higher densities and lower temperatures not only screening but also band filling becomes important, especially in 2D, where the screening wave number no longer increases with density because of the constant density of states in one sub-band.⁶ The numerical calculations which contain these effects (see Fig. 3) show that the asymptotic inequality $|\Delta E_{g2D}/E_{02D}| < |\Delta E_{g3D}/E_{03D}|$ remains valid also for shorter interparticle distances.

In summary, we have presented measurements and calculations for the density dependence of the band-gap renormalization in 2D EHP in GaAs-GaAlAs structures and compared them with corresponding 3D data. The absolute values of the band-gap shifts in two dimensions are found to be much larger than the corresponding three-dimensional ones for equivalent EHP densities. However, in appropriate Rydberg units the band-gap shift in the 2D EHP is considerably weaker than in the 3D case, as a result of the reduced efficiency of screening in two dimensions. Our results imply that the universal law found previously for the band-gap renormalization in 3D systems breaks down if the dimensionality is changed. It would be interesting to study other 2D semiconductors with different band structures in order to test whether there is a new general law of the band-gap renormalization in 2D systems.

We thank M. Pilkuhn and S. Schmitt-Rink for stimulating discussions. The work has been supported by the Deutsche Forschungsgemeinschaft partly under Contract No. Pi-71/20 and partly through the Sonderforschungsbereich Frankfurt-Darmstadt. Parts of this work were carried out in the framework the European Joint Optical Bistability program, supported by the Commission of the European Communities.

¹P. Vashishta and R. K. Kalia, Phys. Rev. B **25**, 6492 (1982); G. Kirczenow and K. S. Singwi, Phys. Rev. Lett. **41**, 326 (1978); T. L. Reinecke and S. C. Ying, Phys. Rev. Lett. **43**, 1054 (1979).

²Proceedings of the Third Trieste International Centre for Theoretical Physics—International Union of Pure and Applied Physics Semiconductor Symposium, edited by M. H. Pilkuhn, J. Lumin. **30** (1985).

³S. V. Shank, R. L. Fork, R. Yen, J. Shah, B. I. Greene, A. C. Gossard, and C. Weisbuch, Solid State Commun. **47**, 981 (1983).

⁴S. Tarucha, H. Kobayashi, Y. Horikoshi, and H. Okamoto, Jpn. J. Appl. Phys. **23**, 874 (1984); D. Fekete, S. Borenstein, A. Ron. E. Cohen, and R. Burnham, Superlattices Microstructures **1**, 245 (1985).

⁵G. Tränkle, H. Leier, A. Forchel, and G. Weimann, Surf. Sci. **174**, 211 (1986).

⁶S. Schmitt-Rink, C. Ell, H. E. Schmidt, and H. Haug, Solid State Commun. **52**, 123 (1984); S. Schmitt-Rink and C. Ell, J. Lumin. **30**, 585 (1985).

⁷For a recent review see H. Haug and S. Schmitt-Rink, J. Opt. Soc. Am. B **2**, 1135 (1985).

⁸M. Cappizzi, S. Modesti, A. Frova, J. L. Staehli, M. Guzzi, and R. A. Logan, Phys. Rev. B **29**, 2028 (1984); H. Nather and L. G. Quagliano, Solid State Commun. **50**, 75 (1985).

⁹J. C. Maan, G. Belle, A. Fasolino, M. Altarelli, and K. Plogg, Phys. Rev. B **30**, 2253 (1984).

¹⁰M. Altarelli, J. Lumin. **30**, 472 (1985); D. A. Broido and T. L. Reinecke, private communication.

¹¹Comparisons of line-shape analyses using alternatively the realistic valence-band structure or a parabolic approximation with bulk masses yield practically equal plasma densities for the samples investigated in the paper. A parabolic approximation with the "2D masses" at $k=0$ obtained from symmetry consideration ($m_{hh}=0.1m_0$, $m_{lh}=0.21m_0$) leads to a significant underestimate of the plasma density and to line shapes which disagree with the experimental spectra.

¹²P. T. Lansberg, Phys. Status Solidi **15**, 623 (1966).

¹³J. Shah, A. Pinczuk, A. C. Gossard, and W. Wiegmann, Phys. Rev. Lett. **54**, 2045 (1985).

¹⁴Consistent with the parabolic approximation of the hole subbands used in the line-shape analysis, we calculated the Rydberg energy and the effective Bohr radius using the heavy-hole mass of the bulk. This mass represents the complicated valence-band structure best for the investigated well widths and densities.

¹⁵H. Totsuji, J. Phys. Soc. Jpn. **39**, 253 (1975).

¹⁶Y. Kuramoto and H. Kamimura, J. Phys. Soc. Jpn. **37**, 716 (1974).

¹⁷J. Hubbard, Proc. Roy. Soc. London, Ser. A **243**, 336 (1957).